

DynRefer: Delving into Region-level Multimodal Tasks via Dynamic Resolution

Yuzhong Zhao^{1*} Feng Liu^{1*} Yue Liu¹ Mingxiang Liao¹ Chen Gong²
Qixiang Ye¹ Fang Wan^{1†}

¹University of Chinese Academy of Sciences ²University of Virginia

zhaoyuzhong20@mailsucas.ac.cn liufeng20@mailsucas.ac.cn

liuyue171@mailsucas.ac.cn liaomingxiang20@mailsucas.ac.cn

chengong@virginia.edu qxye@ucas.ac.cn wanfang@ucas.ac.cn

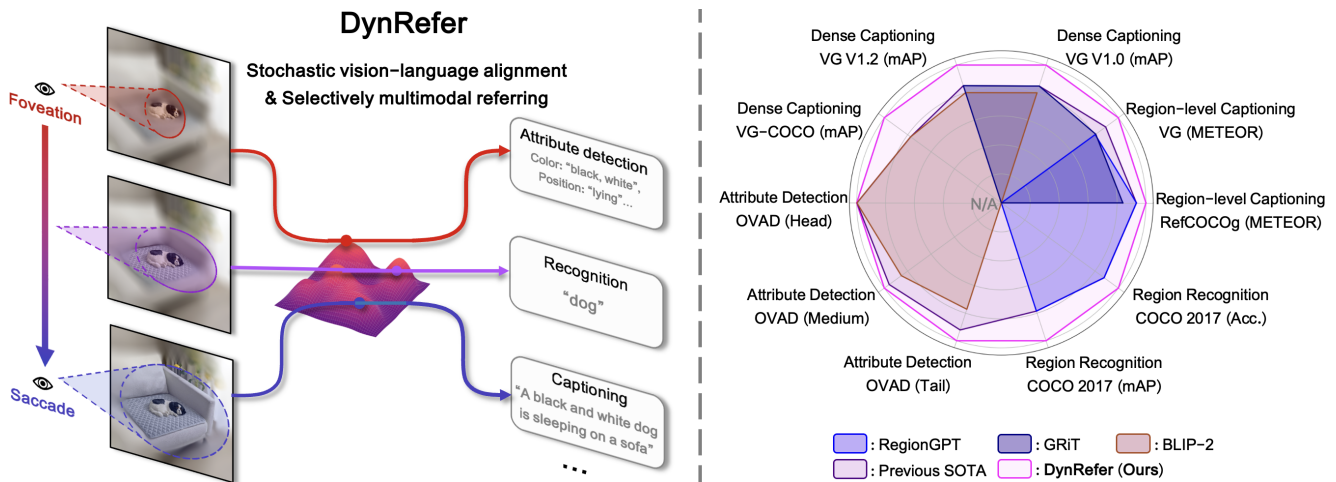


Figure 1. **Left:** Illustration of our DynRefer approach, which dynamically determines proper region views for each task through stochastic vision-language alignment and selectively multimodal referring. **Right:** Performance comparison on region-level multimodal tasks.

Abstract

One fundamental task of multimodal models is to translate referred image regions to human preferred language descriptions. Existing methods, however, ignore the resolution adaptability needs of different tasks, which hinders them to find out precise language descriptions. In this study, we propose a DynRefer approach, to pursue high-accuracy region-level referring through mimicking the resolution adaptability of human visual cognition. During training, DynRefer stochastically aligns language descriptions of multimodal tasks with images of multiple resolutions, which are constructed by nesting a set of random views around the referred region. During inference, DynRefer performs selectively multimodal referring by sampling proper region representations for tasks from the nested views based on image and task priors. This allows the visual information for referring to better match human prefer-

ences, thereby improving the representational adaptability of region-level multimodal models. Experiments show that DynRefer brings mutual improvement upon broad tasks including region-level captioning, open-vocabulary region recognition and attribute detection. Furthermore, DynRefer achieves state-of-the-art results on multiple region-level multimodal tasks using a single model. Code is available at <https://github.com/callsys/DynRefer>.

1. Introduction

Region-level multimodal tasks, as a means of communicating referred information with computer, constitute an important branch of artificial intelligence [4, 15, 22, 62]. These tasks involve translating specific image regions to language descriptions based on task requirements such as open-vocabulary region recognition [39], attribute detection [4, 6], region-level captioning [7, 15, 37, 62]. Existing methods [4, 6, 22, 52, 72] using image regions under fixed

* Equal contribution. † Corresponding Author.

resolution as inputs remain lacking adaptability to capture detailed region information or rich global context.

A naive solution is to increase the resolution of the entire input image to enrich region representations with finer details and broader context. This solution, however, introduces a substantial computational overhead, as popular vision foundation models [12, 14, 21] have already been puzzled by the computational complexity, *e.g.*, $\mathcal{O}(n^2)$ *w.r.t.* the length of input sequence). Additionally, increasing the resolution of input images requires the algorithm to process more irrelevant regions, aggregating the challenge to distinguish useful contextual information from noise.

As a reference, the human visual cognition system can adjust focus of attention through processes like foveation and saccadic eye movements [3, 9], which implies dynamically varying image resolution according to task requirements. For example, Figure 1(left), when identifying attributes of a small region, humans tend to focus their gaze on that specific area (*i.e.*, foveation). When aiming to provide a description of a region within its surrounding context, humans typically scan the area and its environment (*i.e.*, saccade). Different from human perceptual capabilities, multimodal large language models (MLLMs) [5, 15, 27, 62] treat all visual regions equally, which leads to poor encoding of the referred regions and contextual information, hampering model’s adaptability to diverse tasks.

Inspired by dynamic resolution characteristics of the visual cognition system, we propose a *simple-yet-effective* computational approach, DynRefer, to address the adaptability challenge of region-level multimodal tasks, Fig. 1, from the following two perspectives. (i) *Non-uniformity*. The referred region is represented as a high resolution image, while irrelevant regions are either represented as a low resolution image or removed entirely. This forces the model to focus on query relevant regions, leading to better information encoding. (ii) *Adaptability*. The resolution of the image is dynamically adjusted *w.r.t.* the specific language output required by the task. Adaptation enables the model to better align with human preferences. Specifically, it enhances the resolution of the referred region when fine details are required, and improves the resolution of the overall environment when a context-aware description is needed.

DynRefer pursues high-accuracy region-level referring by performing stochastic vision-language alignment during training, and selectively multimodal referring during inference, Fig. 2. For stochastic vision-language alignment, we create images with stochastic resolutions by combining randomly nested image views around the referred region. These images are then embedded and aligned with the desired language descriptions for region-level multimodal tasks. For selectively multimodal referring, we select appropriate image views to form a proper region representation based on task prior and image prior, Fig. 2(lower). When task types

are known in advance, we select views based on the attributes and characteristics of the task. For example, for attribute detection that require fine details, we select contextless but detail-rich views. When task types are unknown, we select views based on image priors by maximizing the total information of the combined views using a greedy search algorithm. This enables the model to generate task-specific outputs aligning with human preferences.

Extensive experiments conducted on OVAD [4], COCO [30], Visual Genome [23], and RefCOCOg [60] show that DynRefer enjoys high representational capacity and strong task adaptability. With a single model, DynRefer is capable of executing multiple tasks and outperforms the state-of-the-art methods in open-vocabulary attribute detection, region recognition, and region-level captioning methods with significant margins, Fig. 1(right). Specifically, DynRefer respectively improves mAP by **1.1%** on OVAD (Open-vocabulary attribute detection), accuracy by **8.8%** on COCO (Open-vocabulary region recognition), mAP by **7.1%** on Visual Genome V1.2 (Dense captioning), and CIDEr by **5.8** on RefCOCOg (Region-level captioning).

The contributions of this study are summarized as follows:

- We propose DynRefer, a simple-yet-effective approach, to pursue high-accuracy region-level referring through mimicking the dynamic resolution mechanism of visual cognition.
- We design a stochastic vision-language alignment procedure to train dynamic resolution models, which constructs the implicit correspondence between dynamic resolution inputs and specific language outputs. We further propose a selectively multimodal referring procedure for dynamic resolution inference, which supports the adaptive prediction of language descriptions for referred regions.
- Experiments on multiple benchmarks show that DynRefer achieves the state-of-the-art results for multiple region-level multimodal tasks using a single model.

2. Related Works

Vision-Language Models. These methods aim to learn multimodal comprehension ability given image-text pairs. Benefiting from powerful foundation models [8, 11, 12, 48, 66] and huge amount of vision-language data corpus [43], VLMs have achieved unprecedented performance across vision-language tasks such as semantic segmentation [53, 70], image-text retrieval [26, 27, 29, 50], visual question answering (VQA) [10, 26, 27, 31], image captioning [10, 26, 27, 31], and few-shot learning [1, 59]. According to the training objectives, VLMs can be categorized into three types: (i) Image-text contrastive learning [21, 39, 50, 59, 72], (ii) Image-text matching [2, 25, 26], and (iii) Language modeling [1, 26, 31, 40, 62]. To accomplish region-level tasks, some of these models [4, 13, 20, 35, 37, 40, 49, 51, 58,

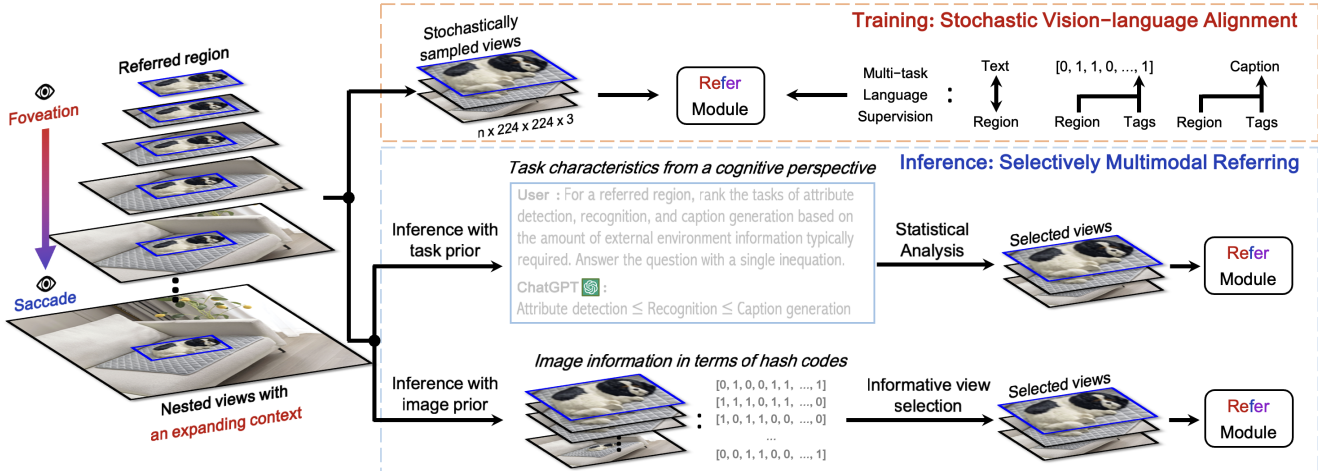


Figure 2. Diagram of the proposed DynRefer. The “dynamic” capability is achieved through a stochastic vision-language alignment procedure during training (upper) and a selectively multimodal referring procedure during reference (lower). During training, the input image is cropped and resized to multiple views surrounding the referred region. The views are then randomly sampled to simulate an image with stochastic resolution. The sampled views are used to train a Refer Module (upper). During inference, the views are sampled based on task and image priors to meet the task requirements and human preference (lower).

62, 68, 72] are trained on region-text pairs to unlock their region-level comprehension ability.

Region-level Multimodal Tasks. The acquisition of preferred semantics (*e.g.*, categories, attributes, captions) for given (referred) image regions is crucial for many multimodal tasks: (i) Region recognition. With the rapid development of VLMs, classifying regions in an open set has become a common practice. The methods based on contrastive learning [21, 33, 39, 72] get the class by calculating the similarity between region embeddings and text embeddings. While the methods based on language modeling [5, 7, 15, 31, 67] query the large language model (LLM) to select the most likely class of given regions among an open set. (ii) Attribute detection. With the release of large-scale attribute datasets including COCO Attributes [36], Visual Genome [23], and VAW [38], recent studies [38, 63] realize attribute detection by training multi-class classification networks. Inspired by CLIP [39], OVAD [4], OvarNet [6] learn to predict attributes from captions, which rely less on densely annotated attributes and can make predictions in an open vocabulary manner. (iii) Region-level captioning. The generation of region-level captions based on large multimodal models (LMMs) has become a widespread practice [7, 37, 40, 47, 62]. GRiT [52] unifies the training of classification and captioning by treating object categories as brief captions. CapDet [33] and DetCLIPv3 [56] further combine dense captioning with open-world detection in a pretraining setup.

The trend of exploiting region-level information for fine-grained vision-language tasks urges the development of res-

olution adaptability, which is crucial to improve the accuracy of recognition, attribute detection, and region-level captioning by dynamically using the context information. Furthermore, for the multiple types of referring tasks, existing methods ignore the inherent similarity between region-level multimodal tasks. There is an urgent requirement to unify these tasks from the perspective of model training. Such unification is expected to bring mutual improvement among tasks so that state-of-the-art results can be achieved for all tasks with a single model.

Dynamic Resolution of Visual Cognition. The research in the visual cognition area has shown that the human vision system has the capability of dynamic resolution. The fovea, situated in the central part of the retina, possesses the highest resolution view, while other parts of the retina dynamically perceive context views for details [9]. Recent research [3] has demonstrated that foveal and peripheral vision are closely linked and differences in appearance between peripheral and foveal vision can be adjusted through re-calibration [46]. In contrast, computer vision systems lack such a dynamic mechanism and instead capture only a static view [16]. To simulate the dynamic resolution mechanism through computer vision is non-trivial.

3. Methodology

The “dynamic” capability is achieved through a stochastic vision-language alignment procedure during training and a selectively multimodal referring procedure during reference, Fig. 2. In the training procedure, we construct a set of nested image views that contain the referred region and

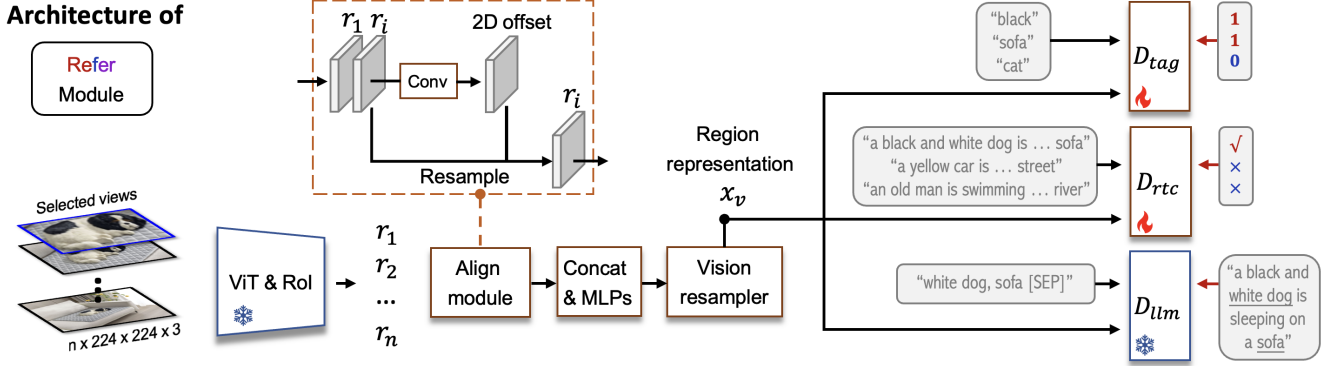


Figure 3. Architecture of the proposed refer module. It comprises a stochastic multi-view embedding module and multimodal decoders (D_*). n nested views are encoded as a region representation x_v by the stochastic multi-view embedding module (left). The region representation x_v is decoded by multimodal decoders, and then aligned to language descriptions of multimodal tasks (right).

randomly sample views to simulate an image with stochastic resolution. A stochastic multi-view embedding procedure is then carried out to encode the image of stochastic resolution to a region representation, which is aligned to language descriptions of multimodal tasks. In the inference procedure, the set of nested image views is constructed once again, and proper views are selected based on task prior and image prior, thereby improving the representational adaptability of region-level multimodal models.

3.1. Training Dynamic Resolution: Stochastic Vision-Language Alignment

3.1.1 Nested View Construction

Vision foundation models, *e.g.*, CLIP and EVA-CLIP [14, 21], are becoming more powerful, but remain handling fixed-resolution images. To exploit their potential for encoding visual inputs of dynamic resolution, we seek a simple alternative by transforming the original image into multiple nested views that cover the referred regions, Fig. 2(left). These nested views share the same resolution and can be combined to simulate an image with dynamic resolution, highlighting the referred region while depressing the irrelevant areas.

Specifically, the original image x is cropped and resized into multiple candidate views. The cropped regions are calculated by $b_r + t * (b_x - b_r)$, $t \in \mathbb{R}[0, 1]$. b_r , b_x , and t respectively denote the bounding box of the referred region, the size of the whole image, and the interpolation coefficient. During training, n views are stochastically sampled from the candidates to simulate images generated by foveation and saccadic eye movements. The n views correspond to interpolation coefficients \mathbf{t} , where $\mathbf{t} = [t_1, t_2, \dots, t_n]$. We keep the view containing only the referred region ($t_1 = 0$) being sampled, *i.e.*, the image with blue border in Fig. 2, which best preserves details and is experimentally validated crucial for all multimodal tasks.

3.1.2 Stochastic Multi-view Embedding

The sampled n views, *i.e.*, image with stochastic resolution, are jointly encoded by a frozen ViT into spatial features, which are further processed by an RoI-Align module [17] to obtain region embeddings, *i.e.*, $\{r_i\}_{i=1,2,\dots,n}$, Fig. 3(left). Due to biases introduced by cropping, resizing, and RoI-Align, the region embeddings are not well spatially aligned. Inspired by dynamic convolution operations [18, 54], we propose an align module (Fig. 3 upper) to reduce the bias by aligning $\{r_i\}_{i=2,3,\dots,n}$ to r_1 , where r_1 is the region embedding that corresponds to the view containing only the referred region. Each region embedding r_i is first concatenated with r_1 , followed by a convolution layer to compute a 2D offset map. The spatial feature of r_i is then resampled according to the 2D offset. Finally, the aligned region embeddings are concatenated across the channel dimension and fused by a multi-layer perceptron (MLP) layer. The outputs are further compressed by a vision resampler, *i.e.*, the Q-former [27], so that we extract a region representation (x_v in Fig. 3) for the referred region b_r of the image x .

3.1.3 Vision-Language Alignment

The region representation x_v , calculated through the stochastic multi-view embedding process, is decoded by three decoders*. D_* is shown in Fig. 3(right), which are respectively supervised by three multimodal tasks:

i) Image Region Tagging. Inspired by the off-the-shelf image tagging methods [19, 32, 69], we apply a query-based lightweight recognition decoder [32] for region tagging. The decoder D_{tag} is shown in Fig. 3(right). This tagging procedure is fulfilled through calculating the confidence of predefined tags by using tags as query and x_v as key and value, respectively. Following the control captioning method [71],

*Please refer to Appendix A for more details about the decoders.

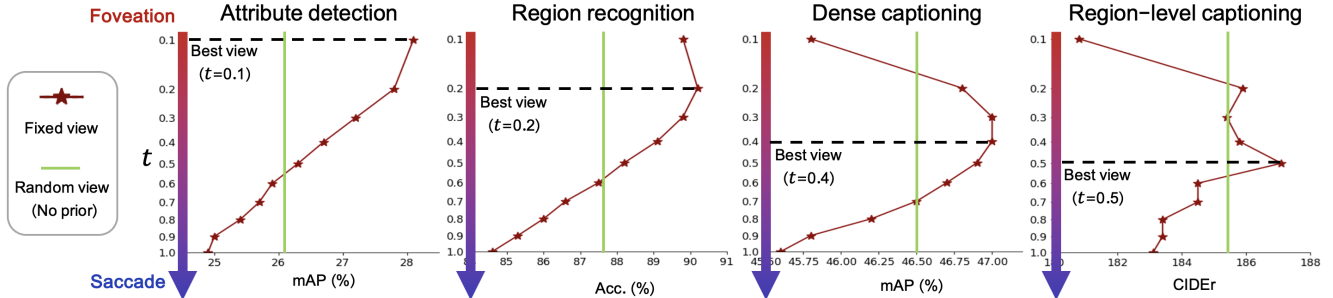


Figure 4. Performance of a double-view ($n = 2$) DynRefer model on region-level multimodal tasks (*e.g.*, open-vocabulary attribute detection on OVAD [4], region recognition on COCO [30], dense captioning on VG-COCO [44], and region-level captioning on VG [23]) under interpolation coefficients \mathbf{t} , $\mathbf{t} = [t_1, t_2] \in \mathbb{R}^2[0, 1]$. The first view is a fixed one ($t_1 = 0$) and the second is randomly selected or fixed.

we parse the ground-truth tags from the captions to supervise the recognition decoder. To handle the problem of missing labels of regions, the asymmetric loss [42], which is robust to imprecise supervision, is used for model optimization.

ii) Region-text Contrastive Learning. Similar to the decoder for region tagging, the decoder D_{rtc} is defined as a query-based recognition decoder [32], which calculates the similarity scores between captions and region features by using the former as the query and the latter as the key and value. This is actually a contrastive learning procedure, where the similarity scores are optimized through the pairwise Sigmoid loss for Language-Image Pre-training [65]. Unlike standard contrastive learning with softmax normalization, the sigmoid loss operates solely on image-text pairs and does not require a global view of the pairwise similarities for normalization.

iii) Language Modeling. As shown in Fig. 3(right), a language modeling decoder D_{llm} is used to convert region representation x_v to language descriptions. Following the typical design of LLMs [27, 31], a learnable linear projector is used to map x_v to the language space. Together with the mapped x_v , random control embeddings[†] [71] built upon word pieces parsed from the ground-truth captions are fed to a frozen LLM for text generation. The language outputs are supervised by the ground-truth captions with a cross-entropy loss [27, 31, 71].

3.2. Inference Dynamic Resolution: Selectively Multimodal Referring

During inference, the trained DynRefer model performs multimodal referring on images with dynamic resolutions. By adjusting the interpolation coefficients \mathbf{t} ($\mathbf{t} = [t_1, t_2, \dots, t_n]$) for the sampled n views, we obtain region representations with dynamic resolution characteristics. This is consistent with the training procedure. The key challenge in multimodal referring is how to adjust the interpolation coefficients \mathbf{t} of the views to select the best view. To this end, we propose two solutions for the two distinct cases, Fig. 2(lower).

[†]More details of the control embeddings are provided in Appendix B.

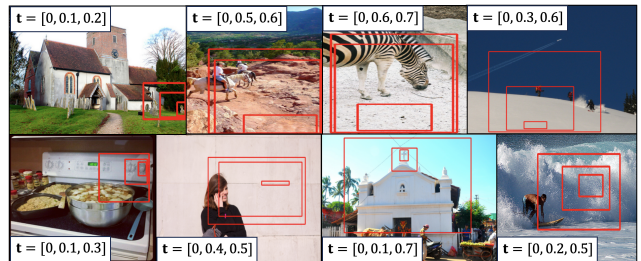


Figure 5. Visualization of selected views using image prior.

i) Inference with task prior: When task prior is known in advance, views are selected based on the specific attributes and characteristics of the task. To investigate the characteristics of existing region-level multimodal tasks, we train a double-view ($n = 2$) DynRefer model and evaluate it on four tasks. From the curves in Fig. 4, we can conclude that better results are achieved for attribute detection under contextless views ($t_2 = 0.1$), which refer to image views tightly bound to the referred region. This is understandable, as such tasks typically require detailed region-specific information. For region-level captioning and dense captioning, context-rich views ($t_2 = 0.4$ or $t_2 = 0.5$) provide better results, as these tasks rely on a more comprehensive context for a fuller understanding of the referred region. It is worth noting that views with excessive context ($t_2 > 0.5$) degrade performance across all tasks, as they introduce too much irrelevant information from outside the region of interest. Thus, by understanding the characteristics of region-level multimodal tasks, one can choose the appropriate views that effectively encode the necessary region representation for each task.

ii) Inference with image prior: When task prior is unknown, views are selected based on image priors by maximizing the total information provided by the combined views using a greedy search algorithm. Specifically, we first construct a set of candidate views with different interpolation coefficients t , $t \in \{0.1, 0.2, \dots, 1\}$. Among these candidates, the first view $x(t_1)$, which contains only the referred

Table 1. Region-level captioning performance of DynRefer and the state-of-the-art methods on the RefCOCOg and VG datasets.

Method	Model size	RefCOCOg		VG	
		METEOR	CIDEr	METEOR	CIDEr
SLR+Rerank _{CVPR'17} [61]	<1B	15.9	66.2	-	-
GPT4RoI _{ARXIV'23} [67]	7.4B	-	-	17.4	145.2
GRIT _{ECCV'24} [52]	<1B	15.2	71.6	17.1	142.0
Groma _{ECCV'24} [34]	7.4B	16.8	107.3	19.0	158.4
ControlCap _{ECCV'24} [71]	4.2B	17.0	111.4	20.4	181.9
Kosmos-2 _{ICLR'24} [37]	1.6B	14.1	62.3	-	-
RegionGPT _{CVPR'24} [40]	7.4B	16.9	109.9	17.0	145.6
GLaMM _{CVPR'24} [40]	7.4B	16.2	106.0	19.7	180.5
Alpha-CLIP _{CVPR'24} [47]	7.4B	16.7	109.2	18.9	160.3
Osprey _{CVPR'24} [62]	7.3B	16.6	108.3	-	-
DynRefer (Ours)	4.2B	18.1	115.7	21.2	190.9

Table 2. Open vocabulary attribute detection performance of DynRefer and the state-of-the-art methods on the OVAD dataset with the box-oracle setup (OVAD-Box).

Method	Backbone	OVAD-Box			
		All	Head	Medium	Tail
Chance [4]	-	8.6	36.0	7.3	0.6
CLIP _{ICML'21} [39]	ResNet50	15.8	42.5	17.5	4.2
CLIP _{ICML'21} [39]	ViT-B16	16.6	43.9	18.6	4.4
Open CLIP _{ICML'21} [21]	ResNet50	11.8	41.0	11.7	1.4
Open CLIP _{ICML'21} [21]	ViT-B16	16.0	45.4	17.4	3.8
Open CLIP _{ICML'21} [21]	ViT-B32	17.0	44.3	18.4	5.5
ALBEF _{NeurIPS'21} [25]	ViT-B16	21.0	44.2	23.9	9.4
X-VLM _{ICML'22} [64]	Swin-B	28.1	49.7	34.2	12.9
OVAD-Baseline _{CVPR'23} [4]	ViT-B32	21.4	48.0	26.9	5.2
BLIP2 _{ICML'23} [27]	EVA	25.5	49.8	30.5	10.8
DynRefer (Ours)	ViT-L	28.2	50.9	34.5	12.5
DynRefer (Ours)	EVA	29.2	49.9	35.7	14.0

region, is always included. In what follows, the remaining $n - 1$ views are selected using a greedy search algorithm. The objective function for the search is formulated as:

$$\operatorname{argmax}_{t_i} \frac{\sum (\text{pHASH}(x(t_1)) \oplus \text{pHASH}(x(t_i)))}{t_i}, \quad (1)$$

where $x(t_i)$ represents the i -th view and t_i denotes its interpolation coefficient. The term “ $\sum (\text{pHASH}(x(t_1)) \oplus \text{pHASH}(x(t_i)))$ ” quantifies the incremental information introduced by the i -th view compared to the first view. The perceptual image hash function, “pHASH(\cdot)” encodes the views into hash codes in the frequency domain, and the XOR operation “ \oplus ” is applied to compare the hash codes of the $x(t_1)$ and $x(t_i)$, capturing the difference in information. The factor “ $\frac{1}{t_i}$ ” serves to downweight context-rich views ($t_i > 0.5$), reducing the risk of introducing redundant information, as observed in Fig. 4. This ensures that the search prioritizes views with balanced and informative content[‡]. The visualizations of selected views based on

[‡]Please refer to Appendix C for the illustration of pHASH operation.

Table 3. Dense captioning performance of DynRefer and the state-of-the-art methods on the VG and VG-COCO datasets. When requiring localization, we use a pre-trained GRIT [52] model to provide bounding boxes.

Method	GT localization	mAP(%)		
		VG V1.0	VG V1.2	VG-COCO
FCLN _{CVPR'16} [22]	✗	5.4	5.2	-
JIVC _{CVPR'17} [55]	✗	9.3	10.0	-
ImgG _{AAAI'19} [28]	✗	9.3	9.7	-
COCD _{AAAI'19} [28]	✗	9.4	9.8	7.9
COCG _{AAAI'19} [28]	✗	9.8	10.4	8.9
CAG-Net _{CVPR'19} [57]	✗	10.5	-	-
TDC _{TNNLS'22} [44]	✗	11.5	11.9	11.9
CapDet _{CVPR'23} [33]	✗	-	15.4	14.0
DCMSTRD _{TMM'24} [45]	✗	13.6	13.4	16.1
GRIT _{ECCV'24} [52]	✗	15.5	16.4	-
ControlCap _{ECCV'24} [71]	✗	18.2	18.5	18.4
PixelLLM _{CVPR'24} [41]	✗	17.0	-	-
DetCLIPv3 _{CVPR'24} [56]	✗	-	19.7	18.9
DynRefer (Ours)	✗	19.1	19.5	19.4
FCLN _{CVPR'16} [22]	✓	27.0	-	-
JIVC _{CVPR'17} [55]	✓	33.6	-	-
CAG-Net _{CVPR'19} [57]	✓	36.3	-	-
BLIP2 _{ICML'23} [27]	✓	37.7	37.9	36.9
GRIT _{ECCV'24} [52]	✓	40.0	40.3	-
ControlCap _{ECCV'24} [71]	✓	42.4	42.8	43.2
DynRefer (Ours)	✓	47.2	47.4	47.6

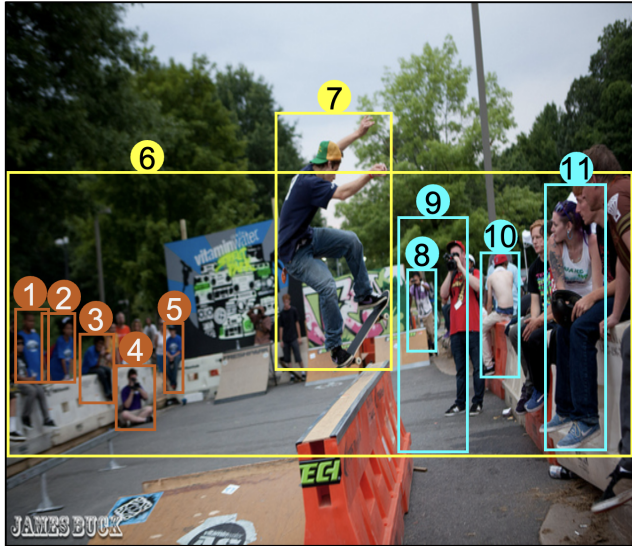
Table 4. Open vocabulary region recognition performance of DynRefer and state-of-the-art methods on the COCO-2017 val set. Following RegionGPT [15] and RegionCLIP [72], we report the results of object classification given ground-truth boxes.

Method	Backbone	LLM	mAP	Acc. (%)
CLIP _{ICML'21} [39]	ViT-L	-	58.9	-
RegionCLIP _{CVPR'22} [72]	R50	-	58.3	-
LLaVA _{NeurIPS'23} [31]	ViT-L	Vicuna-7B	-	40.0
Shikra _{ARXIV'23} [7]	ViT-L	Vicuna-7B	-	53.9
GPT4RoI _{ARXIV'23} [67]	ViT-L	LLaVA-7B	-	64.0
PVIT _{ARXIV'23} [5]	ViT-L+R50	LLaVA-7B	-	64.5
ASM _{ICLR'24} [51]	ViT-L	Hasky-7B	69.3	-
RegionGPT _{CVPR'24} [15]	ViT-L	Vicuna-7B	70.0	80.6
DynRefer (Ours)	ViT-L	FlanT5_{XL}-3B	85.0	89.4
DynRefer (Ours)	EVA	FlanT5_{XL}-3B	89.2	91.8

the image prior are shown in Fig. 5. When the referred region contains minimal information (*e.g.*, a white wall or the ground), the proposed strategy selects more informative views to complement the region.

4. Experiment

DynRefer is implemented upon the LAVIS [24] framework, where vision transformer, vision resampler and large language model are respectively initialized by EVA [14], Q-former [27] and FlanT5_{XL} [8] by default unless otherwise specified. All the sampled views are resized to 224×224



Outputs of DynRefer
In the format of [Category], [Attributes], [Tags], [Caption]

- ① [Person], [clothes color: blue, maturity: adult, order: messy, position: vertical, group: single, gender: male], [blue, boy, person, man, shirt, t shirt], [A man in a blue t shirt].
- ② [Person], [clothes color: blue, maturity: adult, order: messy, group: single, gender: male], [black, blue, boy, wall, cap, hat, person, man, shirt, t shirt, white], [A man in a blue t shirt with a white hat leaning against a wall].
- ③ [Person], [clothes color: blue, maturity: adult, order: messy, position: sitting, group: single, gender: male], [blue, boy, wall, person, jeans, man, shirt], [A person in a blue shirt and jeans sitting on a wall].
- ④ [Person], [clothes color: violet, order: messy, position: sitting], [camera, photographer, person, man, picture, purple, shirt], [A man in a purple shirt taking a picture with a camera].
- ⑤ [Person], [clothes color: blue, maturity: young, order: messy, position: sitting, gender: male], [blue, boy, hat, person, man, shirt, t shirt, truck], [A person wearing a blue t shirt and a black hat].
- ⑥ [Person], [group: group], [crowd, man, skateboard, spectator], [A crowd of spectators watching a man].
- ⑦ [Person], [clothes color: blue, maturity: adult, cleanliness: clean, group: single, state: on, gender: male], [blue, boy, cap, green, hat, jeans, man, ramp, shirt, skateboard, skateboarder, trick, yellow], [A man in a blue shirt and jeans doing a skateboard trick on a ramp].
- ⑧ [Person], [clothes color: tan, maturity: adult, order: messy, group: single, gender: male], [boy, camera, person, man, pant, pants, photo, picture, purple, shirt, white], [A man in a purple shirt and khaki pants taking a picture].
- ⑨ [Person], [clothes color: red, maturity: adult, gender: male], [boy, camera, cap, photographer, hat, person, man, photo, picture, red, shirt], [A man in a red hat taking a picture of a boy in a blue shirt].
- ⑩ [Person], [clothes color: tan, maturity: young, gender: male], [back, boy, wall, cap, hat, person, man, pant, pants, red, shirt, white], [A shirtless man wearing a red cap and white pants leaning against a wall].
- ⑪ [Person], [hair color: violet, maturity: adult, order: messy, gender: female], [blue, girl, hair, person, jeans, man, purple, shirt, t shirt, tattoo, white], [A person with purple hair wearing a white t shirt and blue jeans].

Figure 6. Illustration of DynRefer’s multi-task capability. It can generate captions, tags, attributes, categories for any referred regions.

Table 5. Referring reasoning performance of Finetuned DynRefer and the state-of-the-art methods on the Ferret-Bench [58].

Method	Model size	Referring Reasoning
Shikra-7B _{ARXIV’23} [7]	7.4B	41.6
Kosmos-2 _{ICLR’24} [37]	1.6B	33.7
Ferret-7B _{CVPR’24} [58]	7.4B	67.3
Osprey _{CVPR’24} [62]	7.3B	67.8
DynRefer (Ours)	4.2B	68.9

resolution. All models can be trained less than 20 hours using 8 NVIDIA A800 GPUs. For performance comparison, we train a triple-view ($n = 3$) DynRefer model and inference with image prior on VG V1.2 [23] (*i.e.*, results in Tab. 1 3 2 4 6). For ablation studies, DynRefer is trained on VG-COCO [44] (*i.e.*, results in Tab. 7). For results on RefCOCOg [60], DynRefer is finetuned on its training set. For referring reasoning, DynRefer is finetuned on the combination of LLaVA and Osprey instruction tuning datasets. Please refer to Appendix D for more details about model/dataset/evaluation settings.

4.1. Performance

Region-level Captioning. In Tab. 1 and Tab. 3, DynRefer is compared with the state-of-the-art (SOTA) methods. DynRefer respectively achieves 18.1 and 21.2 METEOR scores, 115.7 and 190.9 CIDEr scores on RefCOCOg and VG, outperforming the SOTA methods with a much smaller model size (4.2B *vs.* 7B). For dense captioning, DynRefer achieves comparable performance with DetCLIPv3 [56]. When the ground-truth localization is given, DynRefer respectively achieves 47.2%, 47.4% and 47.6% mAPs on VG V1.0, V1.2,

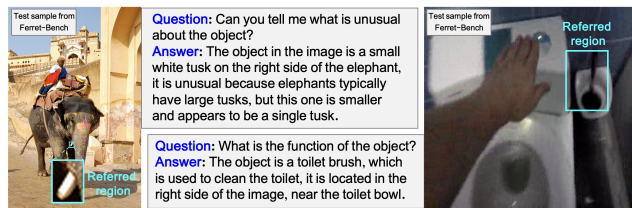


Figure 7. Illustration of finetuned DynRefer’s referring reasoning capability.

and VG-COCO, outperforming GRiT [52] by large margins. **Open-Vocabulary Attribute Detection.** The performance is shown in Tab. 2. DynRefer achieves 29.2% mAP on OVAD, outperforming the SOTA methods. On Medium and Tail attributes, DynRefer achieves the highest mAP, which demonstrates the generalizability of the proposed approach. **Open-Vocabulary Region Recognition.** The performance is shown in Tab. 4. DynRefer outperforms the SOTA methods by large margins (up to 8.8% Acc. and 15% mAP) with a smaller language model. **Referring Reasoning.** The performance is shown in Tab. 5. DynRefer outperforms Osprey [62] by 1.1 (68.9 *vs.* 67.8) with smaller model size (4.2B *vs.* 7B). Some reasoning results of DynRefer are shown in Fig. 7.

Computational Cost and Inference Speed. As shown in Tab. 6, although DynRefer processes more image views, the FLOPs of its vision encoder are comparable to GLaMM [40] and Osprey [62], as each view has a low resolution. DynRefer achieves better region-level captioning performance, with higher METEOR scores on RefCOCOg (17.9 *vs.*, 16.2) and faster inference speed compared to GLaMM [40] (2.55 *vs.* 0.71). These results demonstrate that DynRefer is efficient

Table 6. Comparison of FLOPs of vision encoder (Vis. FLOPs), inference speed (FPS, Frame Per Second), and region-level captioning performance on RefCOCOg between GLaMM [40], Osprey [62] and the proposed approach. FPS is tested on a single A100 GPU. We omit the FLOPs of the language model as it varies with the length of generated sequence. Besides, DynRefer is equipped with FlanT5_{XL}-3B, which is smaller and more efficient than Vicuna-7B.

Method	Backbone	LLM	Vis. FLOPs	FPS	METEOR	CIDEr
GLaMM _{CVPR'24} [40]	ViT-L (Res. 336)	Vicuna-7B	257G	0.71	16.2	106.0
Osprey _{CVPR'24} [62]	ConvNext-L (Res. 512)	Vicuna-7B	200G	2.58	16.6	108.3
DynRefer (Ours)	ViT-L (Res. 224 + Stochastic 3-view)	Vicuna-7B	206G	2.43	17.4	110.7
DynRefer (Ours)	ViT-L (Res. 224 + Stochastic 3-view)	FlanT5 _{XL} -3B	206G	4.81	17.3	109.7
DynRefer (Ours)	EVA (Res. 224 + Stochastic 2-view)	FlanT5 _{XL} -3B	530G	2.55	17.9	114.7

Table 7. Ablation studies of DynRefer on region-level multimodal benchmarks. Line 1: Training with cropped images [27]. Line 2: Training with images with RoI-Align [40, 67]. Lines 3-4: Training with higher resolution images. Line 5: Training with fixed 2-view [71]. Lines 6-11: Training with Stochastic n -view (Ours). Lines 12-18: The effect of removing some core modules or designs in DynRefer. For model inference, “No prior”, “Task prior”, “Image prior” respectively denotes inference with randomly selected views, selection strategies based on task prior and image prior proposed in Sec. 3.2. More details of the ablation studies are provided in Appendix E.

	Training	Inference	Vis. FLOPs	OVAD	COCO	VG-COCO	RefCOCOg	
				mAP (%)	Acc. (%)	mAP (%)	METEOR	CIDEr
1	Cropped image	-	268G	23.0	77.0	40.0	17.1	107.3
2	Image + RoIAlign	-	268G	19.7	74.3	39.1	17.2	110.0
3	Line 2 + Res. 224 → 336	-	618G	21.7	80.1	41.5	17.4	111.3
4	Line 2 + Res. 224 → 448	-	1146G	22.7	81.2	41.8	17.3	113.0
5	Fixed 2-view	-	530G	25.4	85.4	45.8	17.9	114.2
6	Stochastic 2-view	No prior	530G	26.1	87.8	46.6	17.9	114.4
7	Stochastic 2-view	Image prior	530G	27.5	89.3	46.8	17.9	114.7
8	Stochastic 2-view	Task prior	530G	28.1	90.2	47.0	18.1	115.6
9	Stochastic 3-view	No prior	792G	27.3	88.9	47.3	18.2	117.7
10	Stochastic 3-view	Image prior	792G	28.7	90.3	47.4	18.2	118.6
11	Stochastic 4-view	Image prior	1054G	27.2	90.7	47.1	17.8	114.1
12	Line 10 - D_{llm}	Image prior	792G	27.6	89.0	-	-	-
13	Line 10 - D_{rtc}	Image prior	792G	-	-	47.0	18.1	114.2
14	Line 10 - D_{tag}	Image prior	792G	27.0	90.3	44.8	16.7	118.4
15	Line 10 - Pretrained Q-former	Image prior	792G	28.8	90.3	46.7	17.9	113.1
16	Line 10 - ($t_1 = 0$)	Image prior	792G	23.0	74.0	44.4	17.2	110.0
17	Line 10 - Nesting views	No prior	792G	25.5	83.7	43.3	17.5	114.0
18	Line 10 - Align module	No prior	792G	27.3	88.4	47.1	17.9	113.6

and suitable for real-world applications.

4.2. Ablation Studies

Stochastic Multi-view Embedding. In Tab. 7, we compare the proposed stochastic multi-view embedding approach with other commonly used region representation methods [27, 67, 71]. In lines 1-2, the model is trained with resolution-fixed images. In lines 3-4, we increase the resolution of input images based on line 2 following common practice [62], which brings higher FLOPs and limited performance gain. In line 5, the model is trained with visual input of fixed 2-view, which has acceptable FLOPs and large performance gain, demonstrating the efficiency of encoding images of dynamic resolution. In lines 6-8, the views are

stochastically sampled during training, resulting in performance gains across all tasks without extra computational cost, demonstrating the effectiveness of simulating the mechanism of foveation and saccade in human cognition. In lines 9-10, we increase the number of sampled views to 3, which further improves performance at an acceptable cost in terms of FLOPs. However, in line 11, increasing the number of views to 4 leads to a performance drop. This is because with 4 views, there are C_{10}^3 possible combinations of views, which makes the manifold of region representations too complex and harder to optimize.

Vision-Language Alignment. The effectiveness of aligning region representations of images to language descriptions of multi-tasks is validated in lines 12-14, Tab. 7. Dropping

any decoder results in performance degradation, highlighting the mutual improvements among tasks. Aligning without the pretrained Q-former slightly reduces the performance as shown in line 15. Unfixing the view ($t_1 = 0$) significantly harms performance as shown in line 16, demonstrating the importance of the view containing only the referred region, which best preserves details. In line 17, instead of using the strategy of nesting views in Sec. 3.1.2, we randomly select views that contains the referred region during training and inference, which deteriorates the performance. Finally, removing the align module in Fig. 3 slightly reduces the performance on all tasks.

Selectively Multimodal Referring. The effectiveness of selecting views based on task prior and image prior is evaluated in lines 6-10 in Tab. 7. Compared to randomly selected views (No prior) during inference, selecting views based on task prior improve the performance across all tasks as shown in lines 6-8. When task prior is unavailable during inference, selecting views based on image prior is a useful alternative as shown in lines 7-10.

5. Conclusion

We present DynRefer, a resolution-adaptive approach to pursue high-accuracy region-level referring through mimicking the resolution adaptability of human visual cognition. With stochastic vision-language alignment and selectively multimodal referring, DynRefer predicts desired language descriptions for multimodal tasks, as well as customizing the resolution of referred image regions according to the task and image priors. With its powerful adaptability, DynRefer improves the performance of region-level multimodal tasks, with striking contrast to the state-of-the-art methods. Furthermore, DynRefer provides a fresh insight to unify region-level multimodal tasks.

References

- [1] Jean-Baptiste Alayrac, Jeff Donahue, Pauline Luc, Antoine Miech, Iain Barr, Yana Hasson, Karel Lenc, Arthur Mensch, Katherine Millican, Malcolm Reynolds, Roman Ring, Eliza Rutherford, Serkan Cabi, Tengda Han, Zhitao Gong, Sina Samangooei, Marianne Monteiro, Jacob L. Menick, Sebastian Borgeaud, Andy Brock, Aida Nematzadeh, Sahand Sharifzadeh, Mikolaj Binkowski, Ricardo Barreira, Oriol Vinyals, Andrew Zisserman, and Karén Simonyan. Flamingo: a visual language model for few-shot learning. In *NeurIPS*, 2022. 2
- [2] Hangbo Bao, Wenhui Wang, Li Dong, Qiang Liu, Owais Khan Mohammed, Kriti Aggarwal, Subhojit Som, Songhao Piao, and Furu Wei. Vlmo: Unified vision-language pre-training with mixture-of-modality-experts. *NeurIPS*, 35: 32897–32912, 2022. 2
- [3] P. Binda and M. C. Morrone. Vision during saccadic eye movements. *The Journal of Comparative Neurology*, 292(4): 497–523,, 1990. 2, 3
- [4] Maria A Bravo, Sudhanshu Mittal, Simon Ging, and Thomas Brox. Open-vocabulary attribute detection. In *IEEE CVPR*, pages 7041–7050, 2023. 1, 2, 3, 5, 6, 12, 13
- [5] Chi Chen, Ruoyu Qin, Fuwen Luo, Xiaoyue Mi, Peng Li, Maosong Sun, and Yang Liu. Position-enhanced visual instruction tuning for multimodal large language models. *arXiv preprint arXiv:2308.13437*, 2023. 2, 3, 6
- [6] Keyan Chen, Xiaolong Jiang, Yao Hu, Xu Tang, Yan Gao, Jianqi Chen, and Weidi Xie. Ovarnet: Towards open-vocabulary object attribute recognition. In *IEEE CVPR*, pages 23518–23527, 2023. 1, 3
- [7] Keqin Chen, Zhao Zhang, Weili Zeng, Richong Zhang, Feng Zhu, and Rui Zhao. Shikra: Unleashing multimodal llm’s referential dialogue magic. *arXiv preprint arXiv:2306.15195*, 2023. 1, 3, 6, 7
- [8] Hyung Won Chung, Le Hou, Shayne Longpre, Barret Zoph, Yi Tay, William Fedus, Eric Li, Xuezhi Wang, Mostafa Dehghani, Siddhartha Brahma, Albert Webson, Shixiang Shane Gu, Zhuyun Dai, Mirac Suzgun, Xinyun Chen, Aakanksha Chowdhery, Sharan Narang, Gaurav Mishra, Adams Yu, Vincent Y. Zhao, Yanping Huang, Andrew M. Dai, Hongkun Yu, Slav Petrov, Ed H. Chi, Jeff Dean, Jacob Devlin, Adam Roberts, Denny Zhou, Quoc V. Le, and Jason Wei. Scaling instruction-finetuned language models. *arXiv preprint arXiv:2210.11416*, 2022. 2, 6, 12
- [9] C. A. Curcio, Sloan K. R., Kalina R. E., and A. E. Hendrickson. Human photoreceptor topography. *The Journal of Comparative Neurology*, 292(4):497–523,, 1990. 2, 3
- [10] Wenliang Dai, Junnan Li, Dongxu Li, Anthony Meng Huat Tiong, Junqi Zhao, Weisheng Wang, Boyang Li, Pascale Fung, and Steven C. H. Hoi. Instructblip: Towards general-purpose vision-language models with instruction tuning. *arXiv preprint arXiv:2305.06500*, 2023. 2
- [11] Jacob Devlin, Ming-Wei Chang, Kenton Lee, and Kristina Toutanova. BERT: pre-training of deep bidirectional transformers for language understanding. In *NAACL*, pages 4171–4186, 2019. 2
- [12] Alexey Dosovitskiy, Lucas Beyer, Alexander Kolesnikov, Dirk Weissenborn, Xiaohua Zhai, Thomas Unterthiner, Mostafa Dehghani, Matthias Minderer, Georg Heigold, Sylvain Gelly, Jakob Uszkoreit, and Neil Houlsby. An image is worth 16x16 words: Transformers for image recognition at scale. In *ICLR*, 2021. 2
- [13] Debidatta Dwibedi, Vidhi Jain, Jonathan Tompson, Andrew Zisserman, and Yusuf Aytar. Flexcap: Generating rich, localized, and flexible captions in images. *arXiv preprint arXiv:2403.12026*, 2024. 2
- [14] Yuxin Fang, Wen Wang, Binhui Xie, Quan Sun, Ledell Wu, Xinggang Wang, Tiejun Huang, Xinlong Wang, and Yue Cao. Eva: Exploring the limits of masked visual representation learning at scale. In *IEEE CVPR*, pages 19358–19369, 2023. 2, 4, 6
- [15] Qiushan Guo, Shalini De Mello, Hongxu Yin, Wonmin Byeon, Ka Chun Cheung, Yizhou Yu, Ping Luo, and Sifei Liu. Regionpt: Towards region understanding vision language model. In *IEEE CVPR*, pages 13796–13806, 2024. 1, 2, 3, 6, 13

- [16] Strasburger H. even myths on crowding and peripheral vision. *i-Perception*, 11(3):1–46, 2018. 3
- [17] Kaiming He, Georgia Gkioxari, Piotr Dollár, and Ross Girshick. Mask r-cnn. In *IEEE ICCV*, pages 2961–2969, 2017. 4
- [18] Shihua Huang, Zhichao Lu, Ran Cheng, and Cheng He. Fapn: Feature-aligned pyramid network for dense image prediction. In *IEEE ICCV*, pages 864–873, 2021. 4
- [19] Xinyu Huang, Youcai Zhang, Jinyu Ma, Weiwei Tian, Rui Feng, Yuejie Zhang, Yaqian Li, Yandong Guo, and Lei Zhang. Tag2text: Guiding vision-language model via image tagging. *arXiv preprint arXiv:2303.05657*, 2023. 4, 12
- [20] Xiaoke Huang, Jianfeng Wang, Yansong Tang, Zheng Zhang, Han Hu, Jiwen Lu, Lijuan Wang, and Zicheng Liu. Segment and caption anything. In *IEEE CVPR*, pages 13405–13417, 2024. 2
- [21] Gabriel Ilharco, Mitchell Wortsman, Ross Wightman, Cade Gordon, Nicholas Carlini, Rohan Taori, Achal Dave, Vaishaal Shankar, Hongseok Namkoong, John Miller, Hannaneh Hajishirzi, Ali Farhadi, and Ludwig Schmidt. Openclip, 2021. 2, 3, 4, 6, 12
- [22] Justin Johnson, Andrej Karpathy, and Li Fei-Fei. Densecap: Fully convolutional localization networks for dense captioning. In *IEEE CVPR*, pages 4565–4574, 2016. 1, 6, 13
- [23] Ranjay Krishna, Yuke Zhu, Oliver Groth, Justin Johnson, Kenji Hata, Joshua Kravitz, Stephanie Chen, Yannis Kalantidis, Li-Jia Li, David A Shamma, et al. Visual genome: Connecting language and vision using crowdsourced dense image annotations. *IJCV*, pages 32–73, 2017. 2, 3, 5, 7, 13
- [24] Dongxu Li, Junnan Li, Hung Le, Guangsen Wang, Silvio Savarese, and Steven CH Hoi. Lavis: A library for language-vision intelligence. *arXiv preprint arXiv:2209.09019*, 2022. 6, 12
- [25] Junnan Li, Ramprasaath Selvaraju, Akhilesh Gotmare, Shafiq Joty, Caiming Xiong, and Steven Chu Hong Hoi. Align before fuse: Vision and language representation learning with momentum distillation. *NeurIPS*, 34:9694–9705, 2021. 2, 6
- [26] Junnan Li, Dongxu Li, Caiming Xiong, and Steven C. H. Hoi. BLIP: bootstrapping language-image pre-training for unified vision-language understanding and generation. In *ICML*, pages 12888–12900, 2022. 2
- [27] Junnan Li, Dongxu Li, Silvio Savarese, and Steven C. H. Hoi. BLIP-2: bootstrapping language-image pre-training with frozen image encoders and large language models. In *ICML*, pages 19730–19742, 2023. 2, 4, 5, 6, 8, 12
- [28] Xiangyang Li, Shuqiang Jiang, and Jungong Han. Learning object context for dense captioning. In *AAAI*, pages 8650–8657, 2019. 6
- [29] Xiujun Li, Xi Yin, Chunyuan Li, Pengchuan Zhang, Xiaowei Hu, Lei Zhang, Lijuan Wang, Houdong Hu, Li Dong, Furu Wei, et al. Oscar: Object-semantics aligned pre-training for vision-language tasks. In *ECCV*, pages 121–137, 2020. 2
- [30] Tsung-Yi Lin, Michael Maire, Serge Belongie, James Hays, Pietro Perona, Deva Ramanan, Piotr Dollár, and C Lawrence Zitnick. Microsoft coco: Common objects in context. In *ECCV*, pages 740–755, 2014. 2, 5, 13
- [31] Haotian Liu, Chunyuan Li, Qingyang Wu, and Yong Jae Lee. Visual instruction tuning. *NeurIPS*, 36, 2023. 2, 3, 5, 6
- [32] Shilong Liu, Lei Zhang, Xiao Yang, Hang Su, and Jun Zhu. Query2label: A simple transformer way to multi-label classification. *arXiv preprint arXiv:2107.10834*, 2021. 4, 5, 12, 13
- [33] Yanxin Long, Youpeng Wen, Jianhua Han, Hang Xu, Pengzhen Ren, Wei Zhang, Shen Zhao, and Xiaodan Liang. Capdet: Unifying dense captioning and open-world detection pretraining. In *IEEE CVPR*, pages 15233–15243, 2023. 3, 6, 13
- [34] Chuofan Ma, Yi Jiang, Jiannan Wu, Zehuan Yuan, and Xiaojuan Qi. Groma: Localized visual tokenization for grounding multimodal large language models. In *ECCV*, pages 417–435. Springer, 2025. 6
- [35] Ting Pan, Lulu Tang, Xinlong Wang, and Shiguang Shan. Tokenize anything via prompting. *arXiv preprint arXiv:2312.09128*, 2023. 2
- [36] Genevieve Patterson and James Hays. Coco attributes: Attributes for people, animals, and objects. In *ECCV*, pages 85–100, 2016. 3
- [37] Zhiliang Peng, Wenhui Wang, Li Dong, Yaru Hao, Shaohan Huang, Shuming Ma, and Furu Wei. Kosmos-2: Grounding multimodal large language models to the world. *ICLR*, 2024. 1, 2, 3, 6, 7
- [38] Khoi Pham, Kushal Kafle, Zhe Lin, Zhihong Ding, Scott Cohen, Quan Tran, and Abhinav Shrivastava. Learning to predict visual attributes in the wild. In *IEEE CVPR*, pages 13018–13028, 2021. 3
- [39] Alec Radford, Jong Wook Kim, Chris Hallacy, Aditya Ramesh, Gabriel Goh, Sandhini Agarwal, Girish Sastry, Amanda Askell, Pamela Mishkin, Jack Clark, Gretchen Krueger, and Ilya Sutskever. Learning transferable visual models from natural language supervision. In *ICML*, pages 8748–8763, 2021. 1, 2, 3, 6
- [40] Hanoona Rasheed, Muhammad Maaz, Sahal Shaji, Abdelrahman Shaker, Salman Khan, Hisham Cholakkal, Rao M Anwer, Eric Xing, Ming-Hsuan Yang, and Fahad S Khan. Glamm: Pixel grounding large multimodal model. In *IEEE CVPR*, pages 13009–13018, 2024. 2, 3, 6, 7, 8, 13
- [41] Zhongwei Ren, Zhicheng Huang, Yunchao Wei, Yao Zhao, Dongmei Fu, Jiashi Feng, and Xiaojie Jin. Pixellm: Pixel reasoning with large multimodal model. In *IEEE CVPR*, pages 26374–26383, 2024. 6
- [42] Tal Ridnik, Emanuel Ben-Baruch, Nadav Zamir, Asaf Noy, Itamar Friedman, Matan Protter, and Lihi Zelnik-Manor. Asymmetric loss for multi-label classification. In *IEEE CVPR*, pages 82–91, 2021. 5, 12
- [43] Christoph Schuhmann, Romain Beaumont, Richard Vencu, Cade Gordon, Ross Wightman, Mehdi Cherti, Theo Coombes, Aarush Katta, Clayton Mullis, Mitchell Wortsman, et al. Laion-5b: An open large-scale dataset for training next generation image-text models. *NeurIPS*, pages 25278–25294, 2022. 2
- [44] Zhuang Shao, Jungong Han, Demetris Marnerides, and Kurt Debattista. Region-object relation-aware dense captioning via transformer. *IEEE TNNLS*, 2022. 5, 6, 7, 13
- [45] Zhuang Shao, Jungong Han, Kurt Debattista, and Yanwei Pang. Dcmstrd: End-to-end dense captioning via multi-scale

- transformer decoding. *IEEE Transactions on Multimedia*, pages 1–13, 2024. 6
- [46] E. E. M. Stewart and Schütz A. C. Attention modulates trans-saccadic integration. *The Journal of Comparative Neurology*, 142:1–10, 2018. 3
- [47] Zeyi Sun, Ye Fang, Tong Wu, Pan Zhang, Yuhang Zang, Shu Kong, Yuanjun Xiong, Dahua Lin, and Jiaqi Wang. Alpha-clip: A clip model focusing on wherever you want. In *IEEE CVPR*, pages 13019–13029, 2024. 3, 6
- [48] Ashish Vaswani, Noam Shazeer, Niki Parmar, Jakob Uszkoreit, Llion Jones, Aidan N Gomez, Łukasz Kaiser, and Illia Polosukhin. Attention is all you need. *NeurIPS*, 2017. 2
- [49] Teng Wang, Jinrui Zhang, Junjie Fei, Hao Zheng, Yunlong Tang, Zhe Li, Mingqi Gao, and Shanshan Zhao. Caption anything: Interactive image description with diverse multimodal controls. *arXiv preprint arXiv:2305.02677*, 2023. 2
- [50] Wenhui Wang, Hangbo Bao, Li Dong, Johan Bjorck, Zhiliang Peng, Qiang Liu, Kriti Aggarwal, Owais Khan Mohammed, Saksham Singhal, Subhojit Som, and Furu Wei. Image as a foreign language: Beit pretraining for all vision and vision-language tasks. *arXiv preprint arXiv:2208.10442*, 2022. 2
- [51] Weiyun Wang, Min Shi, Qingyun Li, Wenhai Wang, Zhenhang Huang, Linjie Xing, Zhe Chen, Hao Li, Xizhou Zhu, Zhiguo Cao, et al. The all-seeing project: Towards panoptic visual recognition and understanding of the open world. *ICLR*, 2024. 2, 6
- [52] Jialian Wu, Jianfeng Wang, Zhengyuan Yang, Zhe Gan, Zicheng Liu, Junsong Yuan, and Lijuan Wang. Grit: A generative region-to-text transformer for object understanding. In *ECCV*, pages 207–224. Springer, 2025. 1, 3, 6, 7, 13
- [53] Weijia Wu, Yuzhong Zhao, Hao Chen, Yuchao Gu, Rui Zhao, Yefei He, Hong Zhou, Mike Zheng Shou, and Chunhua Shen. Datasetm: Synthesizing data with perception annotations using diffusion models. *NeurIPS*, 2023. 2
- [54] Yuwen Xiong, Zhiqi Li, Yuntao Chen, Feng Wang, Xizhou Zhu, Jiapeng Luo, Wenhai Wang, Tong Lu, Hongsheng Li, Yu Qiao, Lewei Lu, Jie Zhou, and Jifeng Dai. Efficient deformable convnets: Rethinking dynamic and sparse operator for vision applications. *arXiv preprint arXiv:2401.06197*, 2024. 4
- [55] Linjie Yang, Kevin Tang, Jianchao Yang, and Li-Jia Li. Dense captioning with joint inference and visual context. In *IEEE CVPR*, pages 2193–2202, 2017. 6
- [56] Lewei Yao, Renjie Pi, Jianhua Han, Xiaodan Liang, Hang Xu, Wei Zhang, Zhenguo Li, and Dan Xu. Detclipv3: Towards versatile generative open-vocabulary object detection. In *IEEE CVPR*, pages 27391–27401, 2024. 3, 6, 7
- [57] Guojun Yin, Lu Sheng, Bin Liu, Nenghai Yu, Xiaogang Wang, and Jing Shao. Context and attribute grounded dense captioning. In *IEEE CVPR*, pages 6241–6250, 2019. 6
- [58] Haoxuan You, Haotian Zhang, Zhe Gan, Xianzhi Du, Bowen Zhang, Zirui Wang, Liangliang Cao, Shih-Fu Chang, and Yinfei Yang. Ferret: Refer and ground anything anywhere at any granularity. *arXiv preprint arXiv:2310.07704*, 2023. 2, 7
- [59] Jiahui Yu, Zirui Wang, Vijay Vasudevan, Legg Yeung, Mojtaba Seyedhosseini, and Yonghui Wu. Coca: Contrastive captioners are image-text foundation models. *arXiv preprint arXiv:2205.01917*, 2022. 2
- [60] Licheng Yu, Patrick Poirson, Shan Yang, Alexander C Berg, and Tamara L Berg. Modeling context in referring expressions. In *ECCV*, pages 69–85, 2016. 2, 7, 13
- [61] Licheng Yu, Hao Tan, Mohit Bansal, and Tamara L Berg. A joint speaker-listener-reinforcer model for referring expressions. In *IEEE CVPR*, pages 7282–7290, 2017. 6
- [62] Yuqian Yuan, Wentong Li, Jian Liu, Dongqi Tang, Xinjie Luo, Chi Qin, Lei Zhang, and Jianke Zhu. Osprey: Pixel understanding with visual instruction tuning. In *IEEE CVPR*, pages 28202–28211, 2024. 1, 2, 3, 6, 7, 8, 13
- [63] Yu Yun, Sen Wang, Mingzhen Hou, and Quanyue Gao. Attributes learning network for generalized zero-shot learning. *Neural Networks*, 150:112–118, 2022. 3
- [64] Yan Zeng, Xinsong Zhang, and Hang Li. Multi-grained vision language pre-training: Aligning texts with visual concepts. In *ICML*, pages 25994–26009, 2022. 6
- [65] Xiaohua Zhai, Basil Mustafa, Alexander Kolesnikov, and Lucas Beyer. Sigmoid loss for language image pre-training. In *IEEE ICCV*, pages 11975–11986, 2023. 5, 12
- [66] Susan Zhang, Stephen Roller, Naman Goyal, Mikel Artetxe, Moya Chen, Shuohui Chen, Christopher Dewan, Mona T. Diab, Xian Li, Xi Victoria Lin, Todor Mihaylov, Myle Ott, Sam Shleifer, Kurt Shuster, Daniel Simig, Punit Singh Koura, Anjali Sridhar, Tianlu Wang, and Luke Zettlemoyer. OPT: open pre-trained transformer language models. *arXiv preprint arXiv:2205.01068*, 2022. 2
- [67] Shilong Zhang, Peize Sun, Shoufa Chen, Min Xiao, Wenqi Shao, Wenwei Zhang, Kai Chen, and Ping Luo. Gpt4roi: Instruction tuning large language model on region-of-interest. *arXiv preprint arXiv:2307.03601*, 2023. 3, 6, 8
- [68] Tao Zhang, Xiangtai Li, Hao Fei, Haobo Yuan, Shengqiong Wu, Shunping Ji, Chen Change Loy, and Shuicheng Yan. Omg-llava: Bridging image-level, object-level, pixel-level reasoning and understanding. *arXiv preprint arXiv:2406.19389*, 2024. 3
- [69] Youcai Zhang, Xinyu Huang, Jinyu Ma, Zhaoyang Li, Zhaochuan Luo, Yanchun Xie, Yuzhuo Qin, Tong Luo, Yaqian Li, Shilong Liu, et al. Recognize anything: A strong image tagging model. *arXiv preprint arXiv:2306.03514*, 2023. 4, 12, 13
- [70] Yuzhong Zhao, Qixiang Ye, Weijia Wu, Chunhua Shen, and Fang Wan. Generative prompt model for weakly supervised object localization. In *IEEE ICCV*, pages 6351–6361, 2023. 2
- [71] Yuzhong Zhao, Yue Liu, Zonghao Guo, Weijia Wu, Chen Gong, Qixiang Ye, and Fang Wan. Controlcap: Controllable region-level captioning. In *European Conference on Computer Vision*, pages 21–38. Springer, 2024. 4, 5, 6, 8, 12
- [72] Yiwu Zhong, Jianwei Yang, Pengchuan Zhang, Chunyuan Li, Noel Codella, Liunian Harold Li, Luwei Zhou, Xiyang Dai, Lu Yuan, Yin Li, et al. Regionclip: Region-based language-image pretraining. In *IEEE CVPR*, pages 16793–16803, 2022. 1, 2, 3, 6, 13

A. Structure of the Decoders in DynRefer

The structure of the decoders in DynRefer is shown in Fig. 8.

i) Image Region Tagging. As shown in Fig. 8(D_{tag}), the region representation x_v is first mapped to a low-dimension embedding with a linear projection layer. Meanwhile, predefined 4585 tags are encoded by a frozen CLIP [21] text encoder and multi-layer perceptrons. Then, a query-based decoder [32, 69] (“Transformer layers” in Fig. 8) is used to calculate the confidences of the tags. The ground-truth tags are parsed from the caption of the referred region as shown in Fig. 9. Finally, the confidences of the tags are optimized by asymmetric loss [42], which is robust to imprecise supervision.

ii) Region-text Contrastive Learning. As shown in Fig. 8(D_{rtc}), it has a similar structure to D_{tag} . D_{rtc} normalizes the outputs from the query-based decoder and projects them into similarity scores, which are optimized by the pairwise Sigmoid loss for Language-Image Pre-training [65].

iii) Language Modeling. As shown in Fig. 8(D_{llm}), following ControlCap [71], random control words parsed from the ground-truth captions are combined to a sentence, *i.e.*, “white dog, sofa[SEP]”. The sentence is encoded into the control embedding by the tokenizer and word embedding layer of the large language model. After that, a learnable memory unit is added to the control embedding. Finally, the control embedding and the projected region representation are concatenated and jointly sent into the large language model for text generation.

B. Inference with Trained Decoders.

With trained decoders, the region representation x_v can be decoded into region-level language descriptions, including tags, categories, attributes and captions. Their production are elaborated below:

i) tags. The tags of the region are generated by D_{tag} . Following [19, 69], we use a set of 4585 tags. During inference, we first query the decoder with the predefined tags to get the confidences. Then, the tags are filtered by a predefined tagging threshold.

ii) categories. The category of the region is generated by D_{rtc} . During inference, we query the decoder with the template “a photo of a {cls}” and select the category with the highest score.

iii) attributes. The attributes of the region are generated by D_{rtc} . During inference, we first query the decoder with attribute templates following OVAD [4], *e.g.*, “the object has {attr}”. Then, attributes with high scores are selected as the results.

iv) captions. The caption of the region is generated by D_{llm} . During inference, we first use the tags of high confidence to form a control sentence, *i.e.*, “{tag1}, {tag2}, {tag3}, ..., [SEP]”. Then, the control

sentence and the region representation are used to control the language model for caption generation.

C. Details of the Control Embeddings

Following ControlCap [71], we introduce control words to alleviate the caption degeneration issue, which refers to the fact that pre-trained multimodal models tend to predict the most frequent captions but miss the less frequent ones. During training, the control words are parsed from the ground-truth captions (Fig. 9) and are randomly dropped in accordance with a Bernoulli distribution, which is detailed in Fig. 9. The remaining control words are shuffled and combined with a [SEP] token to form a control sentence, *i.e.*, “white dog, sofa[SEP]” in Fig. 8. The sentence is encoded into the control embedding by the tokenizer and word embedding layer of the large language model. During inference, we build the control embeddings with high-confidence tags from the outputs of DynRefer.

D. Illustration of pHASH operation

The pHASH (Perceptual Hash) operation is a hashing algorithm that generates a “perceptual fingerprint” of an image based on its visual characteristics. The key features of pHASH operation are summaries as follows:

i) Perceptual Similarity: The pHASH operation is designed to generate similar hash values for visually similar images. It focuses on the aspects of the image that humans perceive (*e.g.*, shapes, colors).

ii) Tolerance to Minor Modifications: The pHASH operation is robust to minor changes like resizing, cropping, compression, or slight color variations. This tolerance makes it ideal for detecting duplicates or near-duplicates of images.

iii) Fixed-Length Output: The output of the pHASH operation is always a fixed-length binary string (*e.g.*, 64 or 128 bits), regardless of the size of the input image. This makes it easy to compare images of varying sizes.

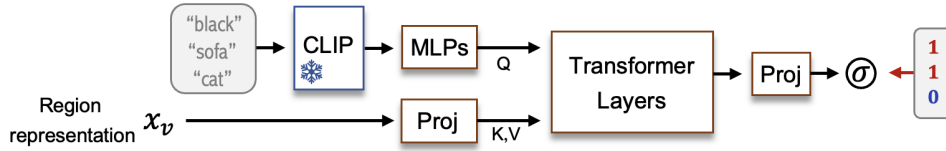
iv) Fast Computation: The pHASH operation is optimized for speed and is computationally efficient, allowing it to be used for large amount image comparisons.

E. Detailed Experimental Settings

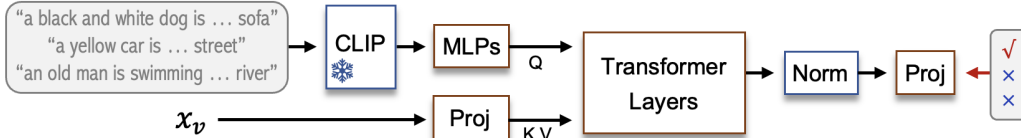
The detailed model, dataset, evaluation settings of DynRefer is summarized as follows:

Model implementation. DynRefer is implemented upon the LAVIS [24] framework, where large language model and vision resampler are respectively initialized by FlanT5_{XL} [8] and Q-former [27]. All the sampled views are resized to 224×224 resolution. All models are trained using 8 NVIDIA A800 GPUs by 5 epochs, with the Adam optimizer where the batch size is set to 512. The total training time is less than 20 hours. The initial learning rate is set to 1×10^{-4}

D_{tag} : Image Region Tagging



D_{rtc} : Region-text Contrastive Learning



D_{llm} : Language Modeling

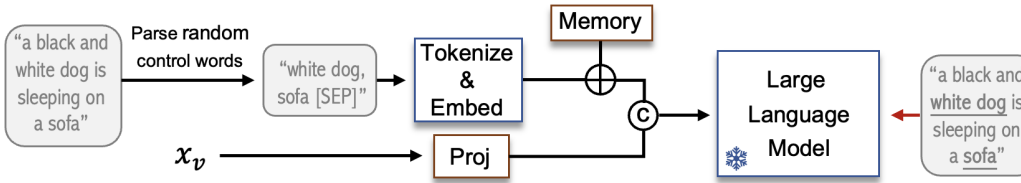


Figure 8. The detailed structure of multimodal decoders D_* of DynRefer. “Proj” is a linear projection layer. “ σ ” is the sigmoid activation function. “Memory” is a learnable embedding. The “Transformer Layers” denotes query-based decoders [32, 69] that contains only cross-attention layers and feed forward networks.

Table 8. Evaluation of the align module of DynRefer on region-level multimodal benchmarks.

	Align module	Inference	Vis. FLOPs	OVAD	COCO	VG-COCO	RefCOCOg	
				mAP (%)	Acc (%)	mAP (%)	CIDEr	METEOR
1	\times	No prior	790G	27.3	88.4	47.1	17.9	113.6
2	\checkmark	No prior	792G	27.3	88.9	47.3	18.2	117.7
3	\times	Image prior	790G	28.1	90.5	46.6	17.7	113.5
4	\checkmark	Image prior	792G	28.7	90.3	47.4	18.2	118.6

with a cosine learning rate decay. The detailed hyperparameters during training and inference are shown in Tab. 11. Considering that dense captioning requires the model to initially generate dense bounding-boxes, we utilize a GRiT [52] model trained on the VG to acquire object locations. During the inference stage, we use the bounding boxes and object scores predicted by GRiT, and then replace its predicted caption with DynRefer to get the final result.

Datasets. For all tasks, DynRefer is trained using Visual Genome (VG) [23] and RefCOCOg [60]. For ablation studies, DynRefer is trained using VG-COCO [44] and RefCOCOg [60]. For evaluation, we evaluate the region-level captioning performance on VG, VG-COCO [44], and RefCOCOg, the open vocabulary attribute detection performance on OVAD [4], and the region recognition performance on COCO [30]

Evaluation Metrics. For region-level captioning, the METEOR score and CIDEr score are adopted as the evaluation metrics following [15, 40, 62]. For dense captioning, mean Average Precision (mAP) [22] is adopted as the evaluation metric following [22, 33]. The mAP is calculated across a range of thresholds for both localization and language accuracy, *i.e.*, the intersection over union (IoU) thresholds (0.3, 0.4, 0.5, 0.6, 0.7) are used for localization and the METEOR score’ thresholds (0, 0.05, 0.1, 0.15, 0.2, 0.25) is adopted for evaluating the language generation. Since DynRefer lacks the capability to perform object detection, we utilize a GRiT [52] model trained on VG to acquire object locations. For open vocabulary attribute detection, mAP is adopted as the evaluation metric following OVAD [4]. For region recognition, mAP and Accuracy (Acc.) are adopted as the evaluation metrics following [15, 72].

Table 9. Evaluation of the inference strategy of DynRefer on region-level multimodal benchmarks.

	Training	Inference	Vis. FLOPs	OVAD	COCO	VG-COCO	RefCOCOg	
				mAP (%)	Acc (%)	mAP (%)	CIDEr	METEOR
1	Stochastic 2-view	No prior	530G	26.1	87.8	46.6	17.9	114.4
2	Stochastic 2-view	Image prior	530G	27.5	89.3	46.8	17.9	114.7
3	Stochastic 2-view	Task prior	530G	28.1	90.2	47.0	18.1	115.6
4	Stochastic 3-view	No prior	792G	27.3	88.9	47.3	18.2	117.7
5	Stochastic 3-view	Image prior	792G	28.7	90.3	47.4	18.2	118.6
6	Stochastic 3-view	Task prior	792G	29.4	90.4	47.4	18.2	118.3

Table 10. Analysis of parameter composition of DynRefer. Modules that contain very few parameters are omitted for clarity.

	ViT	Align module	Vision Resampler	D_{tag}	D_{rtc}	CLIP	LLM
Trainable	✗	✓	✓	✓	✓	✗	✗
Parameters (%)	23.78	0.20	2.53	0.05	0.05	2.99	68.79
Flops (G)	783.5	2.1	6.4	6.2	0.4	6.5	80.1

Image with region caption:
 “a black and white cat is standing on the grass looking at the goldfish in the tank”

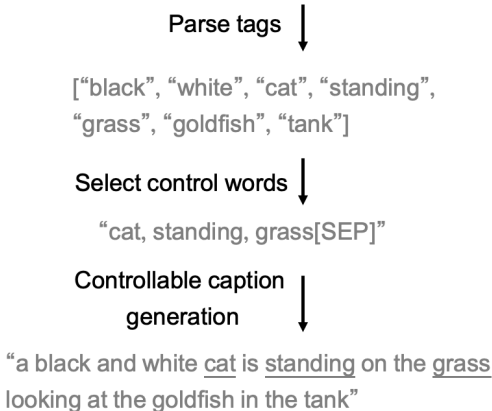


Figure 9. Illustration of the generation process of tags and control words used in DynRefer.

F. Additional Experimental Results

We provide additional experimental results in the supplementary as follows:

Table 11. Detailed hyperparameters during training and inference.

Training	Value
GPUs	8× A800 80G
batch size	512
training epochs	5
learning policy	cosine annealing
initial learning rate	1e-4
minimum learning rate	0
weight decay ratio	0.05
warmup steps	5000
Inference	Value
number of beams	5
number of views	3 (default)
view selection	Image prior (default)

Stochastic Multi-view Embedding: Align module. The effectiveness of the align module is validated in Tab. 8. By spatially aligning the region embeddings across multiple views, DynRefer achieves a 0.6% improvement in mAP on OVAD, a 0.8% improvement in mAP on VG-COCO, and a 5.1 increase in METEOR on RefCOCOg. These results validate the effectiveness of the proposed align module.

Selectively Multimodal Referring. As shown in Tab. 9, we evaluate DynRefer under different view counts and inference strategies. In the “No prior” strategy, views are randomly selected for each sample. In the “Task prior” strategy, the view containing the referred region is always selected, and the top-($n-1$) views are chosen based on the results from Fig. 4 for an n -view model. In the “Image prior” strategy, views are selected according to Eq. 1 in the main paper. For the 2-view DynRefer model, the performance of different strategies ranks as: “Task prior > Image prior > No prior”.

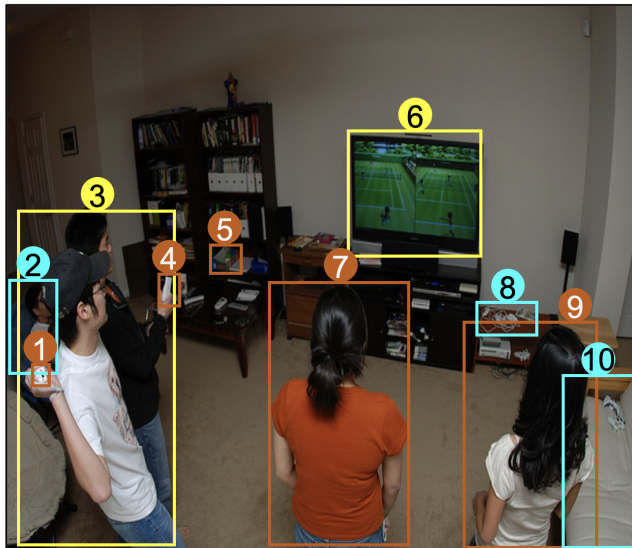
For the 3-view model, the ranking is: “Task prior \approx Image prior $>$ No prior”. While the “Task prior” strategy works well, the “Image prior” strategy offers greater flexibility. It is task-independent and can dynamic select views to each image region. This makes it particularly suitable for models that need to handle multiple tasks with a unified region representation. Based on these advantages, we adopt “Image prior” as the default inference strategy.

Statistics of Parameters and FLOPs. The parameter and flop composition of DynRefer is shown in Tab. 10. DynRefer has few trainable parameters and can be trained efficiently.

Additional Visualization Results. We provide additional visualization results of Fig. 5 and Fig. 6 in the main document. The results are shown in Fig. 12 and Fig. 10 11 13 14 15.

G. Limitations

Though DynRefer significantly outperforms previous state-of-the-arts on multiple multimodal tasks, it still doesn’t perfectly mimic the visual cognition system of human. A real human can adjust the resolution of visual inputs in a more dynamic and flexible way. Better simulation strategy can be explored in the future work.



Outputs of DynRefer

In the format of [Category], [Attributes], [Tags], [Caption]

- ① [Remote], [clothes color: white, cleanliness: clean, size: small, texture: smooth], [black, white, hand, game controller, man, remote, wii], [A white wii remote in the hand of a man].
- ② [Person], [clothes color: white, maturity: young, order: messy, group: single, gender: male, position: horizontal], [blue, boy, couch, game, person, man, shirt, t shirt, white], [A man in a white t shirt sitting on a blue couch watching a game].
- ③ [Person], [clothes color: white, maturity: adult, position: vertical, group: single, gender: male], [black, cap, game, glasses, hat, person, man, shirt, t shirt, white, wii], [A man in a white t shirt with a black cap and glasses playing wii].
- ④ [Remote], [color: white], [hand, man, remote, white, wii, wii controller], [A white wii controller in a man's hand].
- ⑤ [Book], [state: folded, cleanliness: clean, order: messy, material: paper, color quantity: multicolored, group: group], [book, bookcase, bookshelf, notebook, shelf, stack], [A stack of notebooks on a bookshelf].
- ⑥ [TV], [position: horizontal], [game, screen, stand, television, video game, wii], [A television with a wii video game on the screen].
- ⑦ [Person], [clothes color: orange, maturity: young, gender: female], [game, girl, hair, orange, red, shirt, video game, wii, woman], [A woman in an orange shirt playing a video game on the wii].
- ⑧ [Remote], [color: white, order: ordered, texture: smooth, material: polymers, group: group], [table, white, wii], [A white wii controller on a table].
- ⑨ [Person], [maturity: young, gender: female, hair length: long], [black, dark, game, girl, hair, long hair, shirt, white, wii, woman], [A woman in a white shirt with dark long hair watching a game on the wii].
- ⑩ [Couch], [texture: soft, material: polymers], [couch, girl, remote, white, woman], [a white couch behind a woman].

Figure 10. More results of Fig. 6 in the main paper, *i.e.*, illustration of DynRefer's multi-task capability.



Outputs of DynRefer

In the format of [Category], [Attributes], [Tags], [Caption]

- ① [Sink], [order: ordered, material: metal, cooked: raw, texture: smooth, state: piece, optical property: transparent, position: vertical, cleanliness: clean], [basin, counter, kitchen, kitchen sink, sink, white], [A white kitchen sink with a basin on the counter].
- ② [Vase], [pattern: floral, material: glass, cleanliness: clean], [clear, counter, flower, glass vase, vase, window], [A clear glass vase with flowers on the counter].
- ③ [Bowl], [material: ceramic], [bowl, counter, fruit, green, white], [A white bowl with green leaves sitting on the counter].
- ④ [Cup], [order: ordered, color: white, material: ceramic, group: group, optical property: opaque], [coffee cup, counter, cup, mug, white], [A white coffee cup on the counter].
- ⑤ [Spoon], [size: small, order: ordered, texture: smooth, group: single, color quantity: single-colored, optical property: opaque, position: vertical, cleanliness: clean], [wall, hook, ladle, measuring cup, pot, shelf, spoon], [A ladle hanging from a hook on the wall next to a measuring cup and spoon].
- ⑥ [Cup], [material: glass, optical property: transparent, cleanliness: clean], [clear, counter, cup, table, glasses, island, water], [Two clear glasses of water on a wooden counter].
- ⑦ [Refrigerator], [material: metal, state: full], [door, fridge, kitchen], [A refrigerator with two doors in the kitchen].
- ⑧ [Apple], [color: green, cooked: raw, group: group], [apple, bowl, fruit, green, white], [Green apples in a white bowl].

Figure 11. More results of Fig. 6 in the main paper, *i.e.*, illustration of DynRefer's multi-task capability.

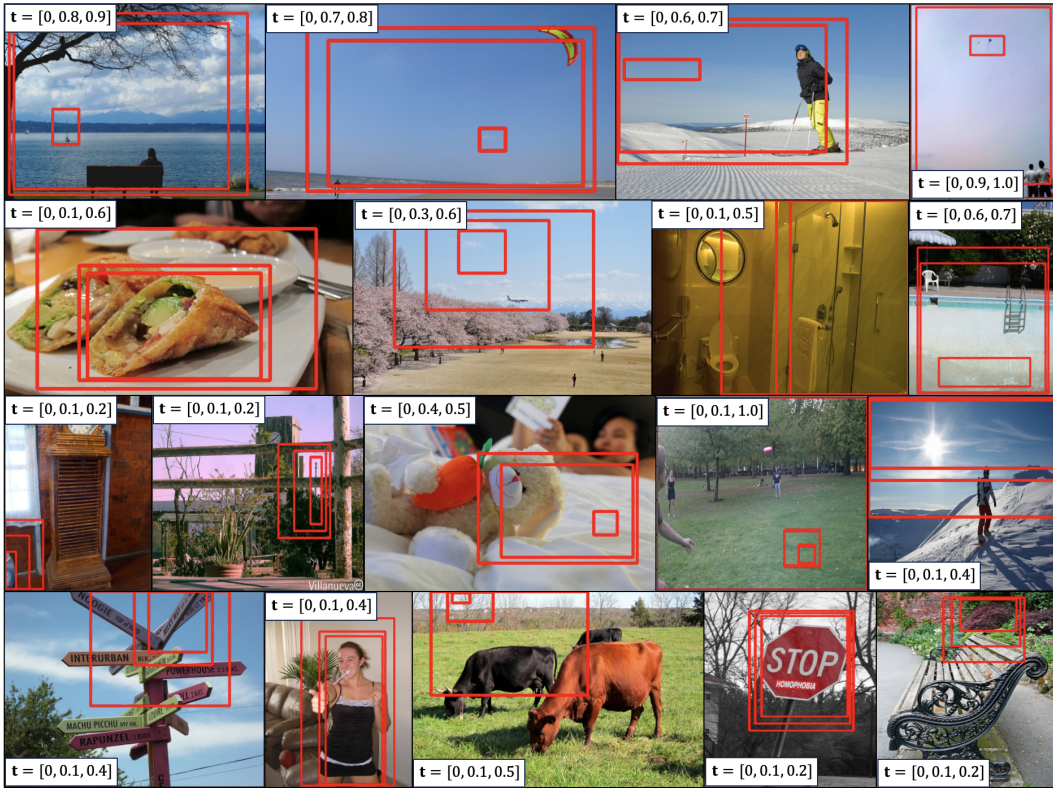


Figure 12. More results of Fig. 5 in the main paper, *i.e.*, visualization of selected views using image prior.

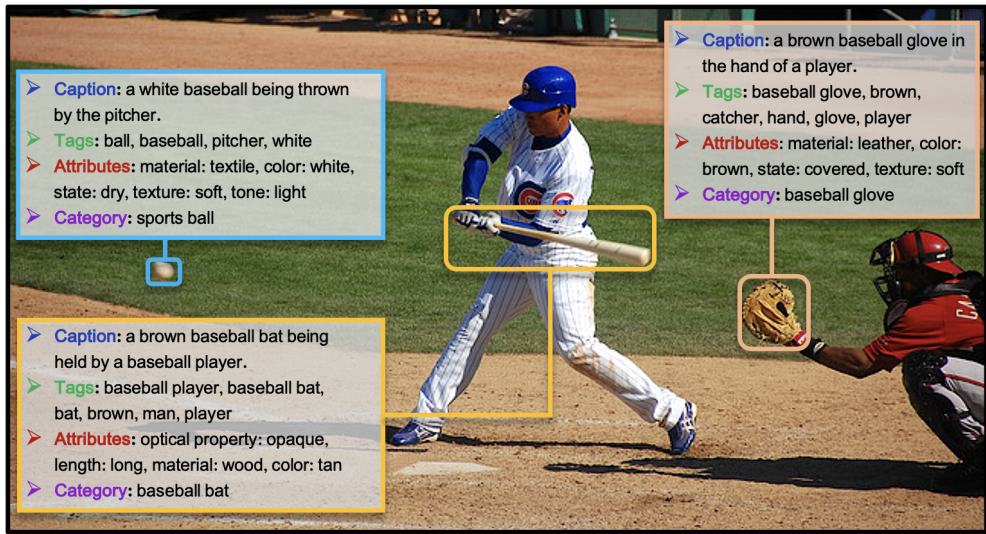


Figure 13. Illustration of DynRefer’s multi-task capability. It can generate captions, tags, attributes, categories, using a single model, for any referred regions.



Figure 14. Illustration of DynRefer's multi-task capability. It can generate captions, tags, attributes, categories, using a single model, for any referred regions.

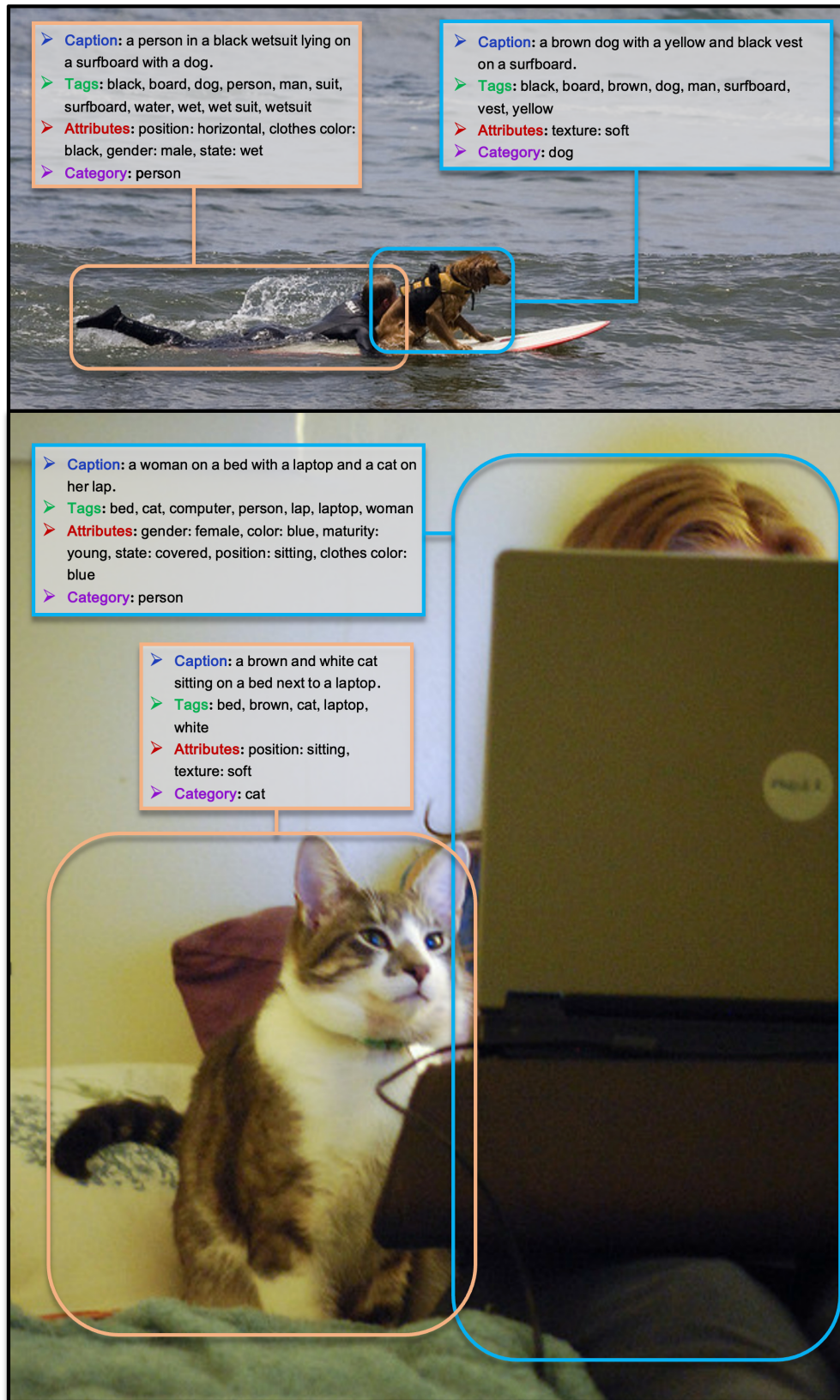


Figure 15. Illustration of DynRefer’s multi-task capability. It can generate captions, tags, attributes, categories, using a single model, for any referred regions.